



**HAL**  
open science

## Viscosity of carbon nanotubes water based nanofluids: Influence of concentration and temperature

Salma Halelfadl, Patrice Estellé, Bahadir Aladag, Nimeti Doner, Thierry Maré

### ► To cite this version:

Salma Halelfadl, Patrice Estellé, Bahadir Aladag, Nimeti Doner, Thierry Maré. Viscosity of carbon nanotubes water based nanofluids: Influence of concentration and temperature. *International Journal of Thermal Sciences*, 2013, 71, pp.111-117. 10.1016/j.ijthermalsci.2013.04.013 . hal-00821792

**HAL Id: hal-00821792**

**<https://hal.science/hal-00821792v1>**

Submitted on 13 May 2013

**HAL** is a multi-disciplinary open access archive for the deposit and dissemination of scientific research documents, whether they are published or not. The documents may come from teaching and research institutions in France or abroad, or from public or private research centers.

L'archive ouverte pluridisciplinaire **HAL**, est destinée au dépôt et à la diffusion de documents scientifiques de niveau recherche, publiés ou non, émanant des établissements d'enseignement et de recherche français ou étrangers, des laboratoires publics ou privés.

1                   **Viscosity of carbon nanotubes water based nanofluids: Influence of**  
2   **concentration and temperature**

3                                   **Salma Halelfadl <sup>a</sup>, Patrice Estellé <sup>b,\*</sup>, Bahadir Aladag <sup>c</sup>,**  
4   **Nimeti Doner <sup>c</sup>, Thierry Maré <sup>a</sup>**

5  
6                   <sup>a</sup> UEB, LGCGM EA3913, Equipe Matériaux et Thermo-Rhéologie, Université Rennes 1, IUT  
7                                   de Rennes, 3 rue du Clos Courtel, BP 90422, 35704 Rennes Cedex 7, France

8  
9                   <sup>b</sup> UEB, LGCGM EA3913, Equipe Matériaux et Thermo-Rhéologie, Université Rennes 1, IUT  
10                                   de Saint-Malo, Rue de la Croix Désilles, CS51713, 35417 Saint-Malo Cedex, France

11  
12                   <sup>c</sup> Department of Mechanical Engineering, Dumlupinar University, 43270 Kutahya, Turkey

13  
14  
15                   \* Author to whom correspondence should be addressed.

16                   Electronic mail: [patrice.estelle@univ-rennes1.fr](mailto:patrice.estelle@univ-rennes1.fr)  
17                   IUT de Rennes, 3 rue du Clos Courtel, BP 90422,

18                   35704 Rennes Cedex 7, France

19                   Tel: +33 (0) 23 23 42 00

20                   Fax: +33 (0) 2 23 23 40 51

21  
22                   **Abstract:**

23  
24                   Experimental results on the steady state viscosity of carbon nanotubes water-based nanofluids  
25                   are presented considering the influence of particle volume fraction and temperature ranging  
26                   from 0 to 40°C. The suspensions consist of multi-walled carbon nanotubes dispersed in de-  
27                   ionized water and they are stabilized by a surfactant. The aspect ratio of nanotubes is close to  
28                   160 and the particle volume fraction varies between 0.0055% and 0.55%. It is shown that the  
29                   nanofluids behave as shear-thinning materials for high particle content. For lower particle  
30                   content, the nanofluids are quite Newtonian. It is also observed that the relative viscosity of  
31                   nanofluids at high shear rate does not vary with temperature. Moreover, the evolution of  
32                   relative viscosity at high shear rate is well predicted by the Maron-Pierce model considering  
33                   the effect of nanoparticles agglomerates.

34  
35  
36  
37                   **Keywords: viscosity, CNT nanofluid, shear-thinning, agglomerates, temperature**

41  
42  
43  
44  
45  
46  
47  
48  
49  
50  
51  
52  
53  
54  
55  
56  
57  
58  
59  
60  
61  
62  
63  
64  
65  
66  
67  
68  
69  
70  
71  
72  
73  
74  
75

**Nomenclature**

- L length of nanotubes
- d average diameter of nanotubes
- r aspect ratio of nanotube, with  $r = L/d$
- $\mu_{bf}$  viscosity of base fluid
- $\mu_{nf}$  viscosity of nanofluid
- $\eta$  intrinsic viscosity
- $\mu_r$  relative viscosity
- $\phi$  nanoparticle volume fraction
- $\phi_m$  maximum packing volume fraction
- $\phi_a$  effective volume fraction of aggregates
- a radius of nanoparticles
- $a_a$  effective radii of aggregates
- D fractal index

**1. Introduction**

Nanofluids are colloidal suspensions containing nanometer-sized particles of metals, oxides, carbides, nitrides, or nanotubes dispersed in a base fluid. The base fluid is usually a conventional fluid such as water, glycol, ethylene glycol, engine oil, etc. Over the past decade, nanofluids have attracted much interest owing to their high thermal conductivity and thermal performance compared to base fluids [1-6]. The thermal enhancement effects and the viscosity of nanofluids are strongly dependent on particle size and concentration, the nature of the base fluid, temperature and the presence of nanoclusters.

From a practical point of view, the viscosity of nanofluids is an important property for applications involving fluid flow and it is used to calculate the required pumping power. The viscosity can change due to the addition of solid nanoparticles and can cause the increase of pressure drops, affecting the efficiency of energy systems. It is also closely related to the stability and the structure of solid nanoparticles. The nanoparticle can agglomerate even at low concentration and also in the presence of a surfactant. In addition, it is well established that the shear-thinning behavior of nanofluids is mainly associated with the shape of nanoparticles and it is enhanced with the presence of nanoparticles agglomerates [7-11].

76 Carbon nanotubes (CNTs) nanofluids have attracted much attention because of their  
77 remarkable properties. Indeed, it was proved that carbon nanotubes nanofluids have a high  
78 thermal conductivity, high electrical conductivity [12,13] and efficient mechanical properties  
79 [14]. The preliminary efforts were to treat and modify the surface of the CNTs to improve  
80 their solubility and to investigate the effect of surfactant and methods to disperse the  
81 nanotubes [15-18]. Nasiri et al. [18] have shown that the CNT structure and stability are  
82 strongly dependant on the functionalization and preparation methods of the nanosuspensions.  
83 The effect of chitosan as a dispersing agent on the viscosity of multi-wall carbon nanotubes  
84 (MWCNTs) dispersed in water was investigated by Phuoc et al. [19]. They showed that the  
85 rheological behavior of nanofluids is affected by both the quantity of chitosan and the CNT  
86 particle content.

87 Garg et al. [20] studied the effect of dispersing energy (ultra-sonication) on the viscosity of  
88 MWCNT aqueous-based nanofluids. They showed that these nanofluids exhibit a shear  
89 thinning behavior which is not related to the presence of the surfactant used. They have also  
90 shown that sonication time is first associated with declustering of nanoclusters CNT  
91 nanofluid. Then, increasing the sonication time breaks the nanotubes leading to less marked  
92 shear-thinning behavior of the nanofluid because of the shorter sizes of the nanotubes. Yang  
93 et al. [21] have also shown the effects of frequency and time of ultrasonication on  
94 agglomerate size and aspect ratio of nanotubes dispersed in oil. They reported that the aspect  
95 ratio of the nanotubes decreases both the dispersing time and the energy increase, resulting in  
96 less viscous nanosuspensions. The shear-thinning behavior of CNT nanofluids was also  
97 observed by Kanagaraj et al. [22]. They have investigated the rheological behavior of CNT  
98 nanofluid under a CNT weight fraction of 1% and for a temperature range of 20 °C to 50°C  
99 and shear rate ranging from 0 to 1000s<sup>-1</sup>. Rheological study of Ponmozhi et al [23] has also  
100 demonstrated the shear-thinning behavior of CNT water-based nanofluids and the viscosity  
101 rise with CNT volume concentration at fixed shear rate and temperature. It was also shown  
102 that CNT water-based nanofluids can behave as a shear time dependent material due to the  
103 time dependency of agglomeration and disagglomeration kinetics under shear, which is linked  
104 to the structural network of the nanofluids [24]. Hence, the rheological behavior of CNT  
105 nanofluids can evolve following its preshear history [25]. The effects of base fluid and  
106 concentration on the rheological behavior of MWCNTs were investigated by Chen et al. [26].  
107 They observed a Newtonian behavior for the studied MWCNTs dispersed in silicone oil,  
108 glycerol or water for all concentrations and temperatures. They also reported the effect of  
109 temperature; the viscosity of nanofluids decreases when the temperature increases.

110 As far as we know, there are few reports of the rheological properties of aqueous CNT  
111 nanofluids. To date, no attempts have been made to interpret the rheological data of such  
112 nanofluids with the presence of particle agglomerates. With this goal, the present paper  
113 reports an experimental investigation of the rheological properties of CNT water-based  
114 nanofluids stabilized by SDBS as surfactant. Here we focus our study on the influence of  
115 particle concentration and temperature. In the first part, we present the CNT water-based  
116 nanofluids used in the study. The experiments for rheological measurements are then detailed  
117 in section 3. In section 4, experimental results are presented and discussed in terms of the  
118 influence of particle content and temperature on the viscosity of CNT suspensions. We  
119 examine various theoretical viscosity models to predict the relative viscosity of CNT  
120 nanofluids at high shear rate and show that it is well represented by the modified Maron-  
121 Pierce equation considering the influence of nanoparticles agglomerates.

122

## 123 **2. Materials**

124

### 125 **2.1 Nanofluid**

126

127 A CNT water-based suspension was provided by Nanocyl (Belgium). According to Nanocyl's  
128 specification, this suspension consists of MWCNTs (carbon purity 90%) dispersed in a base  
129 fluid of de-ionized water and surfactant from ultrasonication, and was stable for several  
130 months. The dimensions of the nanotubes are 1.5  $\mu\text{m}$  in average length  $L$  and 9.2 nm in  
131 average diameter  $d$  respectively. This leads to an average aspect ratio  $r=L/d\approx 163$ . The density  
132 of the nanotubes is  $1800\text{ kg/m}^3$ . The weight fraction of nanotubes is 1%. This corresponds to a  
133 volume fraction of 0.55%. The surfactant used is sodium dodecyl benzene sulfonate (SDBS).  
134 The quantity of surfactant represents 2% of the total weight of the nanosuspension. As it is  
135 well known that carbon nanotubes have a hydrophobic surface, the surfactant is used to  
136 disperse and stabilize the particles and reduce the presence of aggregates [15]. The base fluid  
137 was also independently prepared and provided by Nanocyl.

138

### 139 **2.2 Suspensions preparation**

140 The suspension provided by Nanocyl was used as a starting material to prepare suspensions  
141 with various lower mass concentrations of 0.75, 0.5, 0.2, 0.1, 0.05 and 0.01%. This  
142 corresponds to a volume fraction of 0.418, 0.278, 0.111, 0.055, 0.027 and 0.00555%  
143 respectively. De-ionized water was used to dilute and prepare these suspensions. The  
144 appropriate mass of water was precisely measured and then introduced in the initial

145 suspension to reach the required mass (or volume) fraction in nanotubes. The mixture was  
146 stirred with a mixer for 30min and then remained at rest. The 30min stirring of each  
147 suspension was repeated 24hours later. Mechanical stirring is used to ensure uniform  
148 dispersion of nanoparticles and prevent initial agglomeration of nanoparticles in the base  
149 fluid. Thereafter, all the suspensions were stored in a container at ambient temperature. No  
150 observable sedimentation was noticed before rheological measurements. Following the same  
151 procedure, the initial base fluid was also diluted to obtain the base fluids corresponding to the  
152 different nanofluids previously prepared. The volume fraction of both tested nanofluids and  
153 corresponding base fluids are reported in Table 1.

154

### 155 **3. Experiments**

#### 156 **3.1 Characterization of nanofluids**

157 Scanning Electron Microscopy (SEM) characterization of the starting nanofluid suspension  
158 was preliminary performed to investigate the dispersion state of the nanoparticles within the  
159 base fluid, and evaluate the presence and the size of the aggregates [25]. As reported in Figure  
160 1, it is shown that the nanotubes are entangled and the starting nanofluid suspension is mainly  
161 in the form of aggregates with a maximal aggregate size about 4 times higher than the average  
162 length of the nanotubes.

163

164

#### 165 **3.2 Rheological measurements**

166

167 Rheological measurements of nanofluid samples were performed using a stress controlled  
168 rheometer (Malvern Kinexus Pro) in a cone and plate configuration under controlled  
169 temperature. The temperature was controlled using a Peltier temperature control device  
170 located below the lower plate. Thermal clovers were also used to ensure constant temperature  
171 within the sample gap. For all experiments, the cone diameter was 60mm and the cone angle  
172 was 1°.

173 The working temperature was varied from 0°C to 40°C with an interval of 10°C. The higher  
174 temperature was limited to 40°C because the surfactant addition in nanosuspensions limits  
175 applications at high temperatures [5,6]. It has been shown that above 60°C the bonding  
176 between surfactant and nanoparticles can be damaged [2,4]. The nanofluid will also lose its  
177 stability and sedimentation of nanoparticles will occur [3]. For example, SDBS was observed  
178 to fail at elevated temperatures in [1]. This was also observed from our experiments at 50°C,  
179 as the measured shear viscosity, which varies from one stress to another, indicates the

180 unstable structure under shear (not reported here). The limitation of high temperature was also  
181 used to prevent water evaporation from the sample due to the duration of the rheological  
182 experiments.

183 Each tested volume sample was taken from its container with a syringe-type automatic pipette  
184 and transferred to the lower plate, taking care that no air bubbles were entrapped in the  
185 sample. Hence, the cone is displaced to achieve the required sample gap. The excess of  
186 sample was eventually removed. The sample was allowed to equilibrate for 5 min before  
187 starting the experiment. It should be mentioned that a new sample was used for each  
188 measurement and that both cone and plate were cleaned between each measurement.  
189 Moreover, no high mixing or sonification was applied to the nanofluids before taking it for  
190 rheological measurement. Therefore, no preshear was applied to the samples before testing  
191 them. As a consequence, it is considered that each sample has been subjected to the same  
192 shear history before being tested. Actually, rheological properties of CNT nanofluids are  
193 sensitive to preshear history effect [25].

194 Stress-controlled measurements were performed by imposing a logarithmic stress ramp under  
195 steady-state conditions with maximum step duration of 180s. Once a steady-state flow was  
196 achieved and maintained for 10s, the shear rate was measured. The applicability of the shear  
197 stress range was subject to a preliminary evaluation to ensure steady-state flow at low shear  
198 stress, and to avoid flow instability and sample ejection at high shear stress, in particular for  
199 suspensions with lower mass content in particles. The end value of the shear stress ramp may  
200 vary following the tested suspension, and was set in order to reach a shear rate of  $1000\text{s}^{-1}$  for  
201 each nanosuspension. The experiments were also repeated at least once to both verify the  
202 repeatability of the shear viscosity measurement and the suspension stability with time.

203 Following the same experimental procedure, another series of experiments were conducted to  
204 evaluate the rheological behavior of the base fluids corresponding to the nanofluids with  
205 different volume fraction. The torque resolution of the rheometer is 0.1 nNm. This means that  
206 the uncertainty of shear stress with the cone and plate geometry used is  $1.7 \cdot 10^{-3}$  Pa. The  
207 angular velocity resolution is at least 10 nrad/s. The uncertainty of shear rate, which only  
208 depends on angular velocity and cone angle, is less than  $5.73 \cdot 10^{-7} \text{ s}^{-1}$ . This leads to an  
209 uncertainty in apparent viscosity less than 4% within the shear rate range investigated.

210

## 211 **4. Results and discussion**

212

### 213 **4.1 Viscosity measurement validation and viscosity of base fluids**

214 To evaluate the rheometer uncertainty and the experimental procedure, distilled water was  
215 tested at 20°C following the procedure described here before and for two replicates. As  
216 expected, distilled water exhibits a Newtonian behavior within the shear rate range  
217 investigated. The viscosity value of distilled water was 1.0345, which closely matches with its  
218 theoretical values at 20°C. The relative deviation is less than 3.5%. This is of the same order  
219 of magnitude as the experimental uncertainty.

220 Figure 2 reports the shear viscosity of the base fluid for the starting nanofluid at 0.55% in  
221 volume concentration of nanoparticles. It is observed from figure 2 that this base fluid  
222 behaves in Newtonian manner, as the apparent viscosity is constant within the shear rate range  
223 investigated. The shear viscosity value of this base fluid at 20°C is 1.129mPa.s. This is higher  
224 than the viscosity of de-ionized water, showing the influence of SDBS. It is also shown from  
225 figure 1 that the viscosity of the base fluid decreases when the temperature is increased.

226 The shear viscosity of the base fluid of the nanofluid at 0.0055% in volume fraction of  
227 nanoparticles is reported in figure 3. We observe than this base fluid is also Newtonian as the  
228 shear viscosity is constant within the shear rate range investigated and its viscosity is very  
229 close to the one of de-ionized water. A similar effect of temperature increase is also obtained  
230 for the viscosity of this base fluid. Too, a Newtonian behavior for all tested base fluids is thus  
231 observed.

232 In Table 1, the shear viscosities of all base fluids (corresponding to all tested nanofluids) are  
233 given as a function of volume fraction in SDBS. Table 1 shows that, for all the tested  
234 temperatures, the shear viscosity of base fluids slowly decreases with the decrease of SDBS  
235 volume fraction. This can be explained by the dilution of the base fluids and the reduction of  
236 the presence of SDBS. When the volume fraction of SDBS is lower than 0.169%, the shear  
237 viscosity of the base fluid is quite constant and tends to the viscosity of water. As reported  
238 before, when the temperature increases, the shear viscosity of the base fluids decreases.

239

#### 240 **4.2 Viscosity of nanofluids: Influence of concentration and temperature**

241 Figure 4 reports the evolution of the shear viscosity depending on shear rate for CNT  
242 nanofluid at 0.278% in volume fraction and for all the tested temperatures. Figure 4 shows  
243 that the nanofluid behaves as a shear-thinning fluid as the shear viscosity decreases when the  
244 shear rate increases. The good agreement between two replicates of rheological measurement  
245 for this nanofluid at 10°C can also be noted in figure 4. This shows the repeatability of the  
246 measurement and the stability of the nanofluid. Similar trends were obtained for all nanofluids  
247 and temperatures.



248 In figure 5, the shear viscosity of CNT nanofluid at 0.0055% in volume fraction is plotted  
249 against shear rate. Comparison of figure 4 and 5 shows that the rheological behavior of  
250 nanofluids is strongly dependent on the volume fraction of nanotubes within the nanofluids.  
251 This trend can also be shown by figure 6, when we compare the shear viscosity of all  
252 nanofluids at 20°C. In figure 6 we observe that the higher the concentration, the higher the  
253 shear-thinning behavior and the extent of the shear-thinning region. The transition between  
254 shear-thinning behavior and Newtonian behavior of the nanofluids is for a volume fraction of  
255 0.055%. Figure 5 also shows that the shear viscosity increases with CNT concentration for a  
256 given shear rate. It should be noted that the nanofluid with lower concentration have lower  
257 shear viscosity that of the base fluid. This effect is probably due to the lubricative effect of  
258 nanoparticles [26].

259 It is shown from figures 4 and 5 that temperature has a strong effect on the rheological  
260 properties of CNT nanofluids. Actually, the nanofluids viscosity decreases with increasing  
261 temperature, as generally reported for a wide class of nanofluids and previously observed for  
262 the base fluids.

263 As reported in the literature, the shear-thinning effect, in addition to the effect of nanotubes  
264 length, can be attributed to the disagglomeration of the nanotube clusters and the alignment of  
265 the agglomerates and nanotubes during shear, resulting in less viscous force.

266 It can be noted that the shear-thinning behavior of the studied CNT nanofluids is stronger than  
267 the one reported by Kanagaraj et al. [22], which indicates a great effect of the aspect ratio and  
268 the agglomerates network of the nanotubes on the shear viscosity. In the present work, the  
269 aspect ratio of the nanotubes is higher than the aspect ratio ( $r = L/d \approx 8$ ) of the nanoparticles  
270 used in [22]. Our results are also consistent with the work of Ding et al. [27], which showed  
271 the shear-thinning behavior of aqueous suspension of carbon nanotubes at 20 and 40°C within  
272 the shear rate range 1 to  $1000\text{s}^{-1}$ . Shear-thinning of MWCNT-based aqueous nanofluids was  
273 also observed by Garg et al. [20] at 15 and 30°C for low shear rate range between 0 and  $80\text{ s}^{-1}$   
274 and by Maré et al. [28] for temperatures ranging from 0°C to 10°C.

275 Figure 7 reports the relative viscosity at a high shear rate of  $1000\text{s}^{-1}$ , defined as the ratio of the  
276 CNT nanofluid viscosity at high shear rate to the viscosity of the base fluid at the same shear  
277 rate, as a function of all tested temperatures. While nanofluids and base fluids are strongly  
278 dependent on temperature, it is also observed from figure 7 that the relative viscosity is quite  
279 constant for the tested temperatures under the experimental uncertainty. The relative viscosity  
280 of nanofluids at a high shear rate in function of nanofluid volume fraction is plotted in Figure  
281 8. This figure shows that the viscosity enhancement due to the presence of nanotubes is

282 mainly evidenced for nanoparticles volume fraction of 0.055% and that the viscosity of  
283 nanofluid is 6 times higher than the viscosity of the base fluid for nanoparticles volume  
284 fraction of 0.55%. The influence of volume fraction on the enhancement of relative viscosity  
285 of nanofluids is investigated in the following section, considering first the shape of the  
286 nanotubes and then the presence of agglomerates network.

287

### 288 **4.3 Viscosity models: prediction and comparison with experimental data**

289

290 Some theoretical formulas have been developed to relate the relative viscosity of non-  
291 aggregating colloidal suspensions or nanofluids to particle volume fraction. They are derived  
292 from the pioneering model of Einstein [29]. This model is based on the assumption of viscous  
293 fluid containing non-interacting hard spheres under particle volume fraction less than 1%.  
294

294

$$295 \quad \mu_r = (1 + 2.5\phi) \quad (1)$$

296

297 where  $\mu_r$  is the relative viscosity as defined by the ratio of the viscosity of the nanofluid  $\mu_n$  to  
298 the viscosity of the base fluid  $\mu_{bf}$ , and  $\phi$  is the volume fraction of nanoparticle in base fluid.  
299 Later, Einstein's equation was extended by Brinkman [30] to suspensions with moderate  
300 particle volume fraction, typically less than 4%.

$$301 \quad \mu_r = \frac{1}{(1 - \phi)^{2.5}} \quad (2)$$

302

303 Considering the Brownian motion of nanoparticles and the interaction between a pair of  
304 particles, Batchelor [31] proposed the following equation.

305

$$306 \quad \mu_r = (1 + \eta\phi + k_H\phi^2 + \dots) \quad (3)$$

307

308 In equation (3),  $\eta$  is the intrinsic viscosity and  $k_H$  is the Huggins' coefficient. The values of  $\eta$   
309 and  $k_H$  are 2.5 and 6.5, respectively, for spherical particles.

310

311 For higher particle volume fraction, the Krieger-Dougherty relationship is considered as an  
312 efficient model to relate the viscosity of non-aggregating colloidal suspensions or nanofluids  
313 to particle volume fraction. This relationship is written as follows [32]:

314

315

$$\mu_r = \left(1 - \frac{\phi}{\phi_m}\right)^{-\eta\phi_m} \quad (4)$$

316

317 where  $\eta$  is the Einstein coefficient,  $\eta=2.5$ , and  $\phi_m$  is the particle volume fraction when the  
318 viscosity is infinite, defined as the maximum volume fraction. Typically,  $\phi_m \approx 0.65$  for  
319 random packing of hard spheres.

320 An equation with the same functional form was derived by Maron and Pierce from  
321 consideration of the Ree-Eyring flow equations [33,34]. Noting that equation 5 was obtained  
322 from a minimum principle applied to the energy dissipated by viscous effects.

323

324

$$\mu_r = \left(1 - \frac{\phi}{\phi_m}\right)^{-2} \quad (5)$$

325

326 The previous two equations reduce to the Einstein and Batchelor equations at first and second  
327 order, respectively. The Maron-Pierce equation can also be used to predict the relative  
328 viscosity of fiber suspensions, the maximum volume fraction  $\phi_m$  depending also on the aspect  
329 ratio of the fibers [35]. So, the value of the maximum volume fraction decreases with  
330 increasing aspect ratio. A value of  $\phi_m \approx 0.0361$  is here obtained due to the aspect ratio of the  
331 nanotubes used [35]. This is very low in comparison of the maximum volume fraction of  
332 spheres, thus showing the effect of nanoparticle shape.

333 As mentioned before, many nanoparticles have a non-spherical shape. So Brenner and  
334 Condiff [36] have also developed a viscosity model to consider the shape effects in dilute  
335 suspension. So, for rod-like particles, the Brenner-Condiff equation is applicable for a volume  
336 fraction up to  $1/r^2$  (this corresponds here to 0.004% in volume) and for viscosity at high shear  
337 rate, where  $r$  is the aspect ratio of nanoparticles.

338

339

$$\mu_r = (1 + \eta\phi) \quad (6)$$

340

341 with

342

343

$$\eta = \frac{0.312r}{\ln 2r - 1.5} + 2 - \frac{0.5}{\ln 2r - 1.5} - \frac{1.872}{r} \quad (7)$$

344

345

346 In the presence of agglomerates, it was reported that the relative viscosity of aggregating  
 347 suspensions or nanofluids can be modelled from the application of the fractal concept [37].  
 348 So, the geometry of the aggregates can be described as a fractal like structure with a fractal  
 349 index D. Assuming that the aggregates density change with the radial position and is not  
 350 uniform in the nanofluid [8], the effective volume fraction of nanoparticles, denoted  $\phi_a$ , is  
 351 written as follows

$$\phi_a = \phi \left( \frac{a_a}{a} \right)^{3-D} \quad (8)$$

354 where  $a_a$  and  $a$  are the aggregates and primary nanoparticles radii respectively.

355 This leads to the modified Krieger-Dougherty formula given by equation (9) which was  
 356 successfully applied to model the viscosity enhancement of aggregating nanofluids made of  
 357 spherical particles [11,38] and rod-like particles [8,9,39].

$$\mu_r = \left( 1 - \frac{\phi_a}{\phi_m} \right)^{-\eta\phi_m} \quad (9)$$

362 As a consequence, the modified Maron-Pierce equation can also be written [40]:

$$\mu_r = \left( 1 - \frac{\phi_a}{\phi_m} \right)^{-2} \quad (10)$$

363 As previously reported [8], the fractal index D can depend on the type of aggregation, particle  
 364 size and shape and shear flow condition. So, for aggregating nanofluids with spherical  
 365 particles, D has been reported to be between 1.6 and 2.3 [41-43]. However, a value of 1.8 is  
 366 typically used [40,44]. For aggregating nanofluids with nanorods or nanotubes, D varies  
 367 between 1.5 and 2.45 as reported by [39]. Mohraz et al. [45] showed that the fractal index  
 368 depends on the aspect ratio of nanorods. They reported that D increases from 1.8 to 2.3 for r  
 369 ranging from 1 to 30.6 respectively. A value of 2.1 is generally taken [8,45,46]. Such a value  
 370 was also obtained by Chatterjee and Krishnamoorti [47] for single walled carbon nanotubes  
 371 (SWCNTs) dispersed in PEO, and by Khalkhal and Carreau [48] for MWCNTs dispersed in

376 epoxy resin, and a value of 2.05 was reported by Chen et al. [49] for SWCNTs dispersed in  
377 aqueous suspensions. Based on the above, a value of 2.1 was taken for the fractal index in the  
378 present work.

379 Comparison of the experimental data with the predicted data from the above formulas is  
380 shown in figure 8. It is clear that the Einstein, Brinkman, Brenner and Condiff and Maron-  
381 Pierce formulas cannot predict the relative viscosities of the CNT water based nanofluids for  
382 volume concentration exceeding 0.027%. In addition, the difference between the experimental  
383 and the computed values increases with the volume fraction. This result shows the strong  
384 influence of agglomerates which significantly increase the effective volume of the nanotubes  
385 and thus the relative viscosity of the nanofluid. This also confirms the conclusions reported  
386 previously from the steady state apparent viscosity curves.

387 Nevertheless, figure 8 shows excellent agreement between the prediction of the modified  
388 model of Maron-Pierce and experimental data when  $a_a/a \approx 4.41$ , as the average deviation of  
389 experimental relative viscosity compared to the model is less than 5%. If  $a$  is taken as the  
390 average length of the nanotubes, this leads to a maximum aggregates size close to 6.6 nm,  
391 which is in quite good agreement with the maximum size of CNT aggregates determined from  
392 SEM analyses [25]. A comparison of our results with the data of Chen et al. [38] (EG-  
393 spherical  $\text{TiO}_2$ ,  $d=25\text{nm}$ ,  $a_a/a=3.34$ ,  $D=1.8$ ,  $\phi_m=0.605$ ), the data of Kole and Dey [11] (gear oil-  
394 spherical  $\text{CuO}$ ,  $d=40\text{nm}$ ,  $a_a/a=7.15$ ,  $D=1.7$ ,  $\phi_m=0.605$ ) and the data of Chen et al. [8] (EG-  
395 TNT,  $r \approx 10$ ,  $a_a/a=9.46$ ,  $D=2.1$ ,  $\phi_m=0.3$ ), suggests that the size and the aspect ratio are an  
396 important factor in the formation of nanoclusters within the nanofluids in spite of the use of  
397 surfactant. This shows the influence of particle length on the entanglement of the  
398 nanoparticles, the presence and the size of agglomerates.

399

## 400 **5. Conclusion**

401 We have presented an experimental investigation of the rheological properties of water-based  
402 nanofluids containing carbon nanotubes (CNT) with large aspect ratio. The influence of  
403 particle concentration and temperature on the viscosity of the nanofluids was discussed and  
404 the nanofluids were shown to behave as a shear-thinning material at high particle content. For  
405 lower particle content, the nanofluids behave in Newtonian manner. It was also reported that  
406 temperature affects the viscosity of nanofluids and base fluids but that the relative viscosity of  
407 nanofluids at high shear rate is independent of temperature. The relative viscosity of  
408 nanofluids at high shear rate is strongly enhanced with their particle content showing the

409 presence of aggregates, and can be modelled by the Maron-Pierce equation considering the  
410 influence of nanoparticles agglomerates. An average maximum size of aggregates was thus  
411 evaluated and favourably compared with SEM characterization previously done. The results  
412 of this experimental study also show the relevance of the rheological characterization  
413 concerning the presence and the structural information of nanofluids aggregates and can  
414 contribute to the understanding of the thermal properties of such materials.

415

416

### 417 **Acknowledgments**

418

419 Nanocycl Belgium is gratefully acknowledged for providing the CNT water based nanofluid.

420

### 421 **References**

422

423 [1] D.S. Wen, Y.L. Ding, Effective thermal conductivity of aqueous suspensions of carbon  
424 nanotubes (nanofluids), *J. Thermophys. Heat Transfer* 18 (2004) 481-485.

425

426 [2] M.J. Assael, I.N. Mataxa, J. Arvanitidis, D. Christophilos, C. Lioutas, Thermal  
427 conductivity enhancement in aqueous suspensions of carbon multi-walled and double-walled  
428 nanotubes in the presence of two different dispersants, *Int. J. Thermophys.* 26 (2005) 647-  
429 664.

430

431 [3] X.Q. Wang, A.S. Mujumdar, Heat transfer characteristics of nanofluids: A review, *Int. J.*  
432 *Therm. Sci.* 46 (2007) 1-19.

433

434 [4] S.M.S. Murshed, K.C. Leong, C. Yang, Investigations of thermal conductivity and  
435 viscosity of nanofluids, *Int. J. Therm. Sci.* 47 (2008) 560-568.

436

437 [5] D. Wen, S. Lin, S. Vafaei, K. Zhang, Review of nanofluids for heat transfer applications,  
438 *Particuology* 7 (2009) 141-150.

439

440 [6] D. Wu, H. Zhu, L. Wang, L. Liua, Critical issues in nanofluids preparation,  
441 characterization and thermal conductivity, *Curr. Nanosci.* 5 (2009) 103-112.

442

443 [7] H. Chen, W. Yang, Y. He, Y. Ding, L. Zhang, C. Tan, A.A. Lapkin, D.V.Bavykin, Heat  
444 transfer and flow behaviour of aqueous suspensions of titanate nanotubes (nanofluids),  
445 *Powder Tech* 183 (2008) 63-12.

446

447 [8] H. Chen, Y. Ding, A.A. Lapkin, X. Fan, Rheological behaviour of ethylene glycol-titanate  
448 nanotube nanofluid, *J. Nanopart. Res.* 11 (2009) 1513-1520.

449

450 [9] H. Chen, Y. Ding, A.A. Lapkin, Rheological behaviour of nanofluids containing tube/rod-  
451 like nanoparticles, *Powder Tech.* 194 (2009) 132-141.

452

- 453 [10] S.Q. Zhou, R. Ni, D. Funfschilling, Effects of shear rate and temperature on viscosity of  
454 alumina polyalphaolefins nanofluids, *J. Appl. Phys.* 107 (2010) 054317.  
455
- 456 [11] M. Kole, T.K. Dey, Effect of aggregation on the viscosity of copper oxide-gear oil  
457 nanofluids, *Int. J. Thermal Sci.* 50 (2011) 1741-1747.  
458
- 459 [12] P.J. Harris, Carbon nanotubes and related structures: new materials for the 21<sup>st</sup> century,  
460 Cambridge, University Press, 1999.  
461
- 462 [13] Y. Otsubo, M. Fujiwara, M. Kouno, K. Edamura, Shear-thickening flow of suspensions  
463 of carbon nanofibers in aqueous PVA solutions, *Rheol. Acta* 46 (2007) 905-912.  
464
- 465 [14] M.F. Yu, B.S. Files, S. Arepalli, R.S. Ruoff, Tensile loading of ropes of single wall carbon  
466 nanotubes and their mechanical properties, *Physical Rev Lett* 84 (2000) 5552-5.  
467
- 468 [15] L. Vaisman, H.D. Wagner, G. Marom, The role of surfactants in dispersion of carbon  
469 nanotubes, *Adv. Coll. Int. Sci.* 128-130 (2006) 37-46.  
470
- 471 [16] L. Chen, H. Xie, W. Yu, Nanofluids containing carbon nanotubes treated by  
472 mechanochemical reaction, *Thermoch. Acta* 477 (2008) 21-24.  
473
- 474 [17] H. Wang, Dispersing carbon nanotubes using surfactants, *Curr. Opinion Coll. Interface*  
475 *Sci.* 14 (2009) 364-371.  
476
- 477 [18] A. Nasiri, M. Shariaty-Niasar, A. Rashidi, A. Amrollahi, R. Khodafarin, Effect of  
478 dispersion method on thermal conductivity and stability of nanofluid, *Exp. Thermal Fluid Sci.*  
479 35 (2011) 717-723.  
480
- 481 [19] T.X. Phuoc, M. Massoudi, R.H. Chen, Viscosity and thermal conductivity of nanofluids  
482 containing carbon nanotubes stabilized by chitosan, *Int. J. Thermal Sci.* 50 (2011) 12-18.  
483
- 484 [20] P. Garg, L.A. Jorge, C. Marsh, T.A. Carlson, D.A. Kessler, K. Annamalai, An  
485 experimental study on the effect of ultrasonication on viscosity and heat transfer performance  
486 of multi-wall carbon nanotube-based aqueous nanofluids, *Int. J. Heat Mass Transfer* 52 (2009)  
487 5090-5101.  
488
- 489 [21] Y. Yang, E.A. Grulke, Z.G. Zhanh, G. Wu, Thermal and rheological properties of carbon  
490 nanotube-in-oil dispersions, *J. Appl. Phys.* 99 (2006) 114307.  
491
- 492 [22] S. Kanagaraj, F.R. Varabda, A. Fonseca, J. Ponmozhi, J.A. Lopez da Silva, M.S.A.  
493 Oliveira et al, Rheological study of nanofluids at different concentration of carbon nanotubes,  
494 19th National & 8th ISHMT-ASME Heat Mass Transfer Conf., January 3-5, 2008 hvderabad,  
495 India (paper NFF-7).  
496
- 497 [23] J. Ponmozhi, F.A.M.M. Gonçalves, A.G.M. Feirreira, I.M.A Fonseca, S. Kanagaraj, M.  
498 Martins, M.S.A. Oliveira, Thermodynamic and transport properties of CNT water based  
499 nanofluids, *J. Nano Res.* 11 (2010) 101-106.  
500

501 [24] B. Aladag, S. Halelfadl, N. Doner, T. Maré, S. Duret, P. Estellé, Experimental  
502 investigations of the viscosity of nanofluids at low temperatures, *App. Energy*, 97 (2012)  
503 876-880.  
504

505 [25] P. Estellé, S. Halelfadl, N. Doner, T. Maré, Shear flow history effect on the viscosity of  
506 carbon nanotubes water based nanofluid, *Current Nanoscience*, 9/2 (2013) 225-230.  
507

508 [26] L. Chen, H. Xie, W. Yu, Y. Li, The rheological behaviors of nanofluids containing multi-  
509 walled carbon nanotube, *J. Disp. Sci. Tech.* 32 (2011) 550-554.  
510

511 [27] Y. Ding, H. Alias, D. Wen, R.A. Williams, Heat transfer of aqueous suspensions of  
512 carbon nanotubes (CNT nanofluids), *Int. J. Heat Mass Transfer* 49 (2006) 240-250.  
513

514 [28] T. Maré, S. Halelfadl, O. Sow, P. Estellé, S. Duret, F. Bazantay, Comparison of the  
515 thermal performances of two nanofluids at low temperature in a plate heat exchanger, *Exp.*  
516 *Thermal Fluid Sci* 35 (2011) 1535-1543.  
517

518 [29] A. Einstein, *Investigations on the Theory of the Brownian Movement*, Dover  
519 Publications, Inc., New York, 1956.  
520

521 [30] H.C. Brinkman, The viscosity of concentrated suspensions and solutions, *J. Chem. Phys.*  
522 20 (1952) 571-581.  
523

524 [31] G. Batchelor, The effect of Brownian motion on the bulk stress in a suspension of  
525 spherical particles, *J. Fluid Mech.* 83 (1977) 97-117.  
526

527 [32] I.M. Krieger, T.J. Dougherty, A mechanism for non-Newtonian flow in suspension of  
528 rigid spheres, *J. Trans. Soc. Rheol.* 3 (1959) 137-152.  
529

530 [33] S.H. Maron, P.E. Pierce, Application of Ree-Eyring generalized flow theory to  
531 suspensions of spherical particles, *J. Colloid Sci.* 11 (1956) 80-95.  
532

533 [34] M.M. Cross, Viscosity-concentration-shear rate relations for suspensions, *Rheol. Acta* 14  
534 (1975) 402-403.  
535

536 [35] S. Mueller, E.W. Llewellyn, H.M. Mader, The rheology of suspensions of solid particles.  
537 *Proc. of The Royal Society A*, 466 (2010) 1201-1228.  
538

539 [36] H. Brenner, D.W. Condiff, Transport mechanics in systems of orientable particles. Part  
540 IV. Convective transport, *J. Colloid Int. Sci.* 47 (1974) 199-264.  
541

542 [37] W. Wolthers, M.H.G. Duits, D. van den Ende, J. Mellema, Shear history dependence of  
543 aggregated colloidal dispersions, *J. Rheol.* 40 (1996) 799-811.  
544

545 [38] H. Chen, Y. Ding, C. Tan, Rheological behavior of nanofluids, *New J. Phys.* 9 (2007)  
546 367.  
547

548 [39] H. Chen, S. Witharana, Y. Jin, C. Kim, Y. Ding, Predicting thermal conductivity of  
549 liquids suspensions of nanoparticles (nanofluids) based on rheology, *Particuology* 7 (2009)  
550 151-157.



551  
552 [40] J. Chevalier, O. Tillement, F. Ayela, Structure and rheology of SiO<sub>2</sub> nanoparticle  
553 suspensions under very high shear rates, *Phys Rev E* 80 (2009) 051403.  
554  
555 [41] T.D. Waite, J.K. Cleaver, J.K. Beattie, Aggregation kinetics and fractal structure of  
556 gamma-alumina assemblages, *J. Colloid Int. Sci.* 241 (2001) 333–339.  
557  
558 [42] B.X. Wang, L.P. Zhou, X.F. Peng, A fractal model for predicting the effective thermal  
559 conductivity of liquid with suspension of nanoparticles, *Int. J. Heat Mass Transf.* 46 (2003)  
560 2665–2672.  
561  
562 [43] Y. Xuan, Q. Li, W. Hu, Aggregation structure and thermal conductivity of nanofluids,  
563 *AIChE J.* 49 (2003) 1038–1043.  
564  
565 [44] R. Prasher, P.E. Phelan, P. Bhattacharya, Effect of aggregation kinetics on the thermal  
566 conductivity of nanoscale colloidal solutions (nanofluid), *Nano Lett.* 6 (2006) 1529.  
567  
568 [45] A. Mohraz, D.B. Moler, R.M. Ziff, M.J. Solomon, Effect of monomer geometry on the  
569 fractal structure of colloidal rod aggregates, *Phys. Rev. Lett.* 92 (2004) 155503.  
570  
571 [46] J.M. Lin, T.L. Lin, U. Jeng, Y. Zhong, C. Yeh, T. Chen, Fractal aggregates of the Pt  
572 nanoparticles synthesized by the polyol process and poly(N-vinyl-2-pyrrolidone) reduction, *J.*  
573 *Appl. Crystallogr.* 40 (2007) 540-543.  
574  
575 [47] T. Chatterjee, R. Krishnamoorti, Dynamic consequences of the fractal network of  
576 nanotube-poly(ethylene oxide) nanocomposites, *Phys. Rev. E Stat. Nonlinear Soft Matter*  
577 *Phys.* 75 (2007) 050403.  
578  
579 [48] F. Khalkhal, P.J. Carreau, Scaling behavior of the elastic properties of non-dilute  
580 MWCNT-epoxy resin, *Rheol. Acta* 50 (2011) 717-728.  
581  
582 [49] Q. Chen, C. Saltiel, S. Manickavasagam, L.S. Schadler, R.W. Siegel, H. Yang ,  
583 Aggregation behavior of single-walled carbon nanotubes in dilute aqueous suspension, *J.*  
584 *Colloid Interface Sci.* 280 (2004) 91-97.  
585

586 **Figure Captions**

587

588 Figure 1. SEM image taken from dried starting nanofluid [25] (This figure was reprinted with  
589 the permission of Bentham Science Publishers)

590

591 Figure 2. Apparent shear viscosity of the base fluid corresponding to the nanofluid with  
592 0.55% in CNT volume fraction – Influence of temperature.

593

594 Figure 3. Apparent shear viscosity of the base fluid corresponding to the nanofluid with  
595 0.0055% in CNT volume fraction– Influence of temperature.

596

597 Figure 4. Apparent shear viscosity of nanofluid with 0.278% in CNT volume fraction –  
598 Influence of temperature.

599

600 Figure 5. Apparent shear viscosity of nanofluid with 0.0055% in CNT volume fraction –  
601 Influence of temperature.

602

603 Figure 6. Viscosity of nanofluids at 20°C as a function of shear rate for different volume  
604 fraction of nanotubes.

605

606 Figure 7. Relative viscosity of nanofluids as a function of particle volume content and  
607 temperature.

608

609 Figure 8. Relative viscosity of nanofluids as a function of particle volume content and  
610 temperature - Comparison of experimental data and viscosity models.

611

612

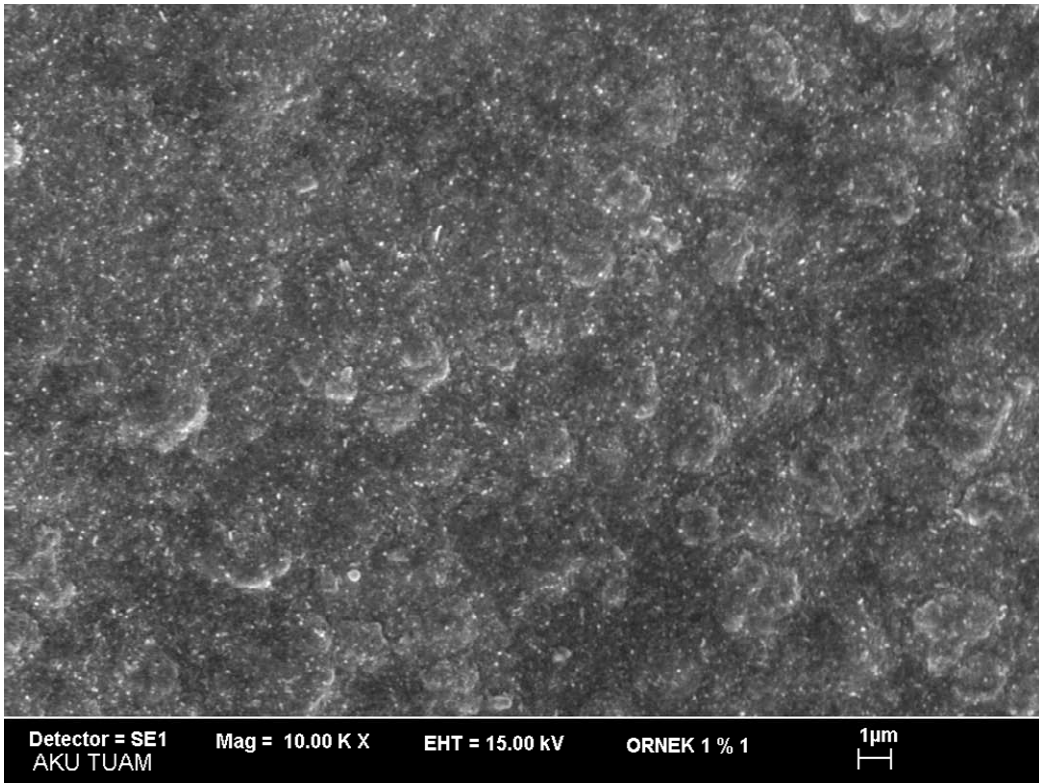
613 **Table Caption**

614

615 Table 1. Volume fraction of tested nanofluids and corresponding base fluids, and shear  
616 viscosity of base fluids as a function of SDBS volume fraction and temperatures.

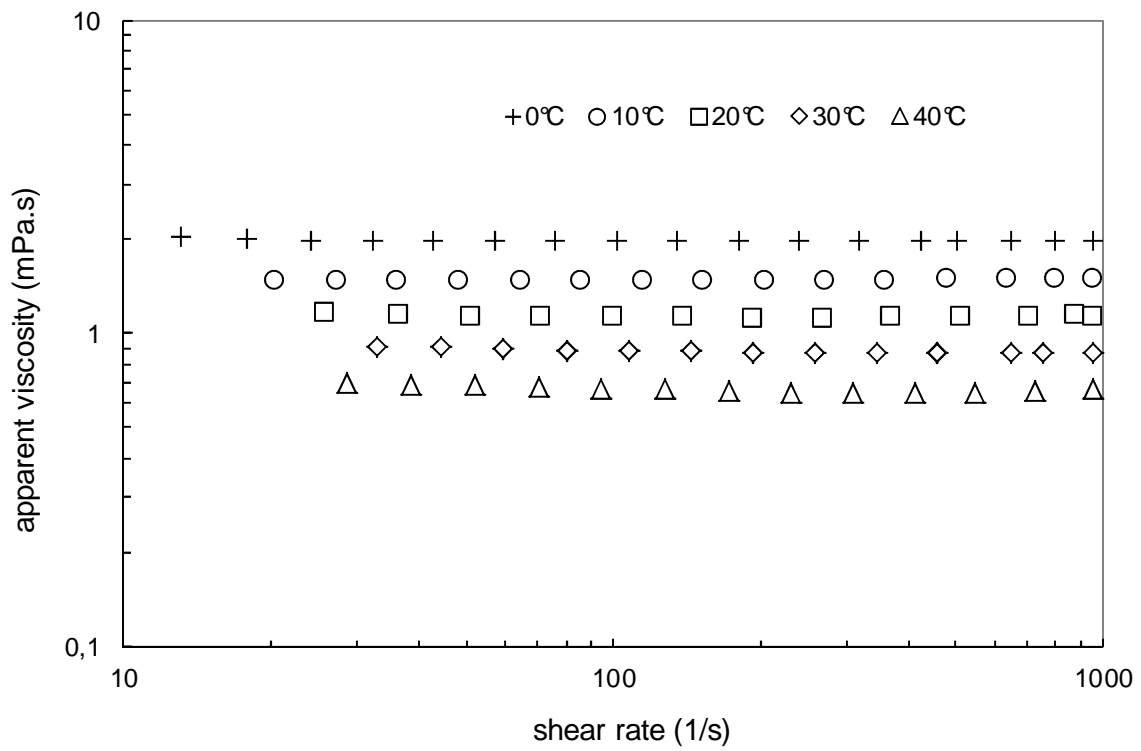
617

618



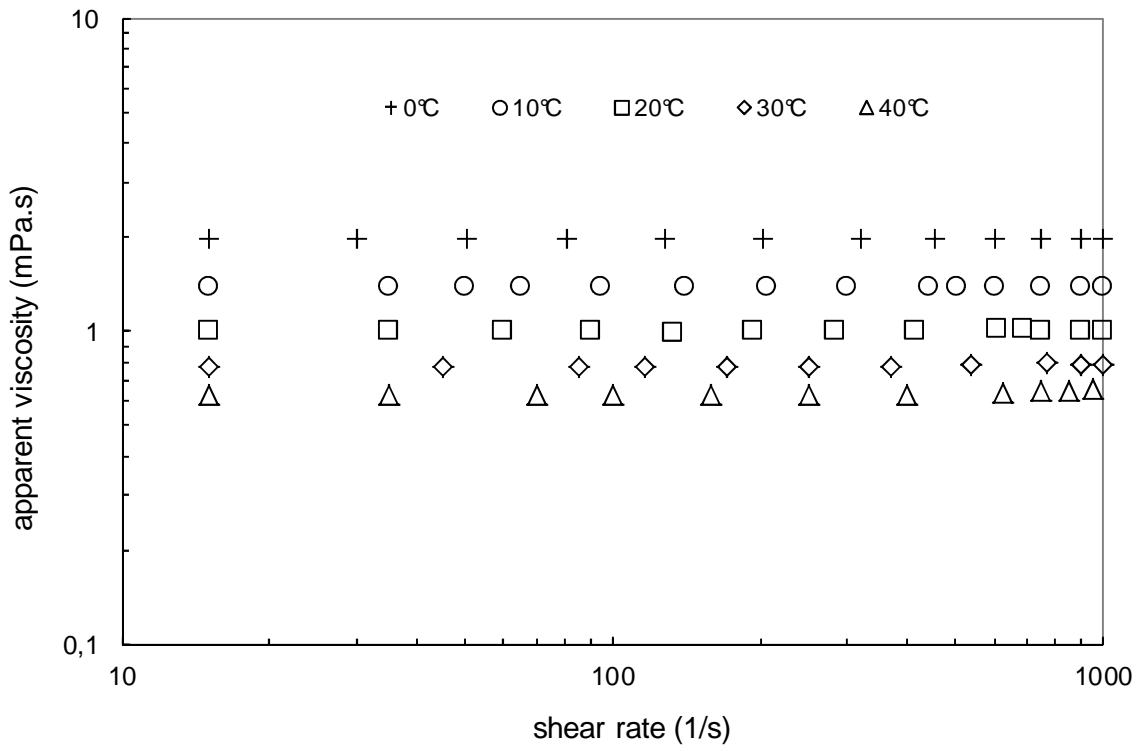
619  
620  
621  
622  
623  
624  
625

Figure 1. SEM image taken from dried starting nanofluid [25] (This figure was reprinted with the permission of Bentham Science Publishers)

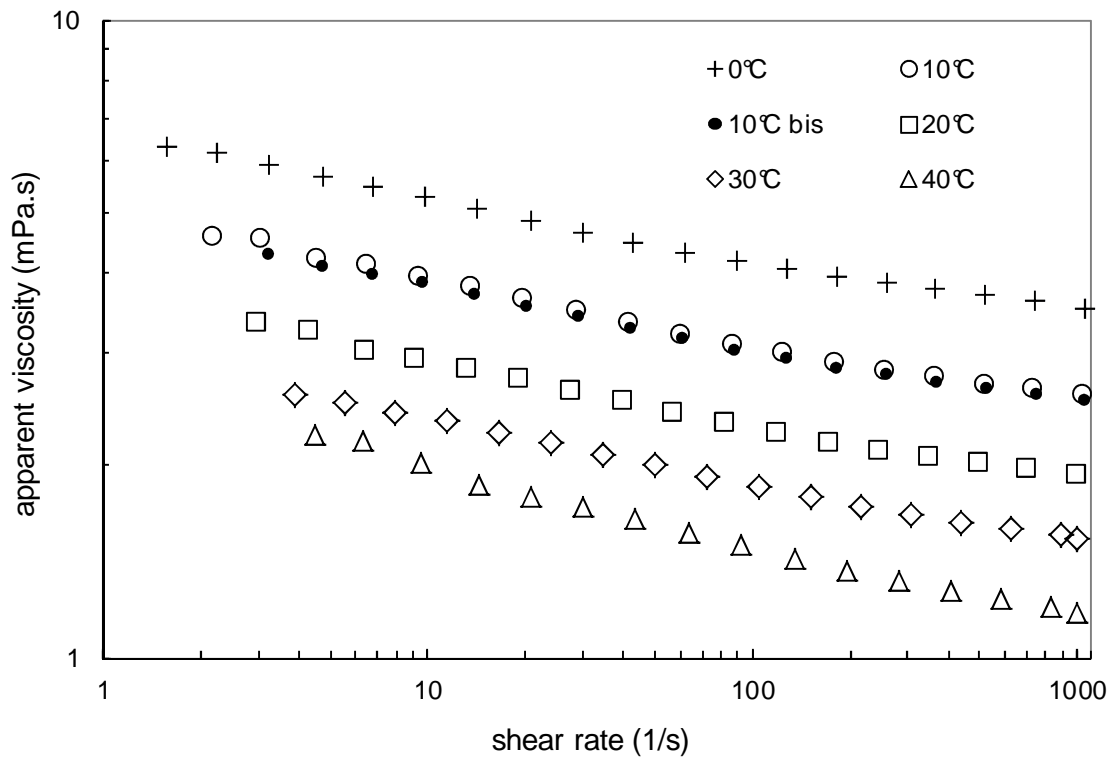


627  
628  
629  
630

Figure 2. Apparent shear viscosity of the base fluid corresponding to the nanofluid with 0.55% in volume fraction – Influence of temperature.

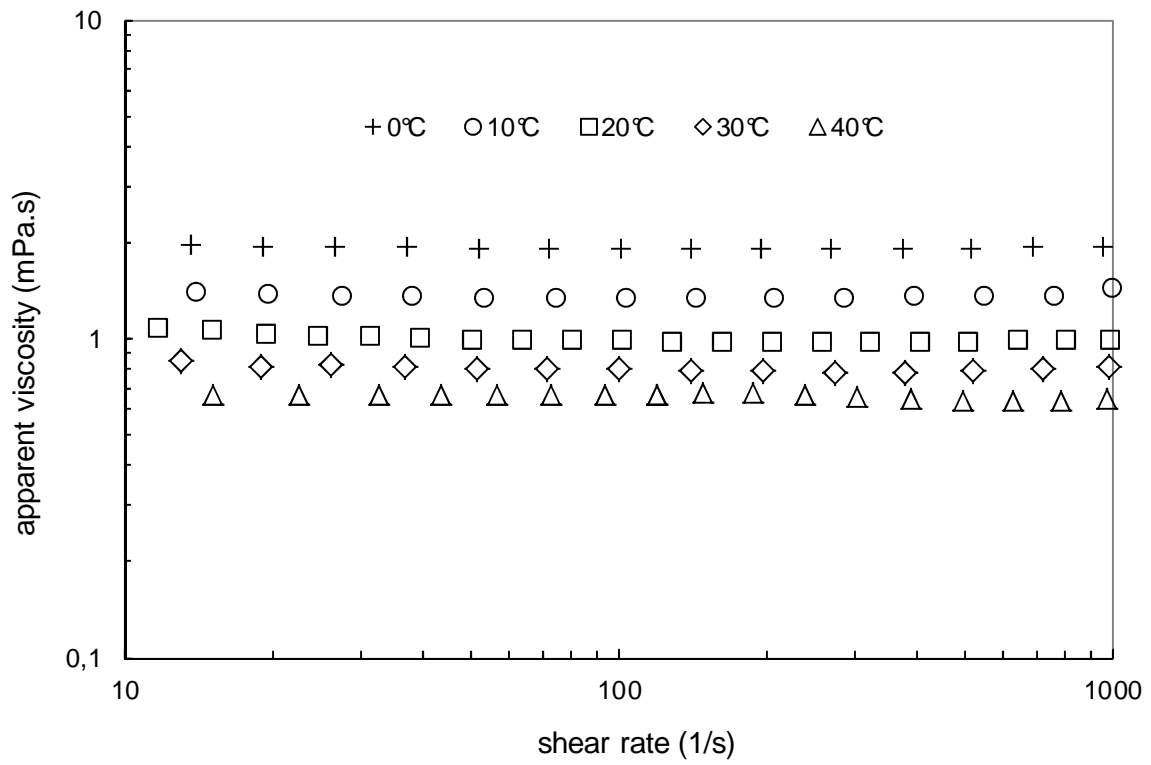


632  
 633 Figure 3. Apparent shear viscosity of the base fluid corresponding to the nanofluid with  
 634 0.0055% in volume fraction– Influence of temperature.  
 635  
 636

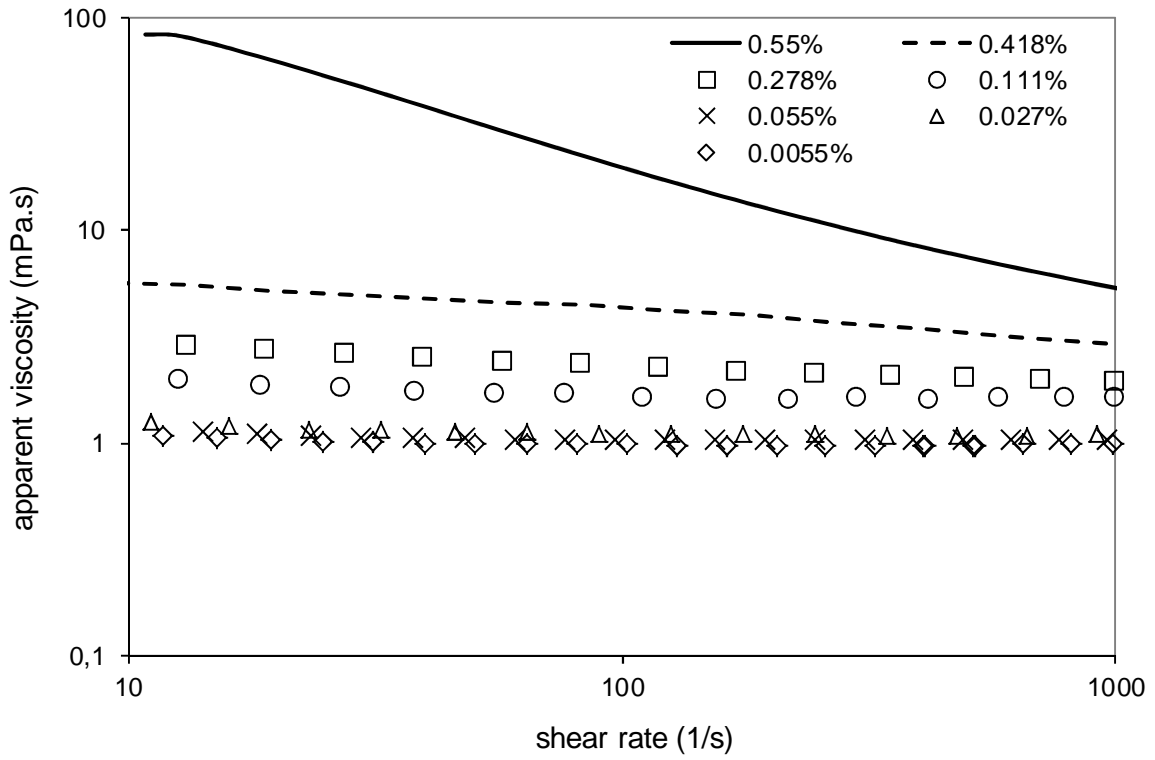


638  
 639  
 640  
 641

Figure 4. Apparent shear viscosity of nanofluid with 0.278% in CNT volume fraction – Influence of temperature.

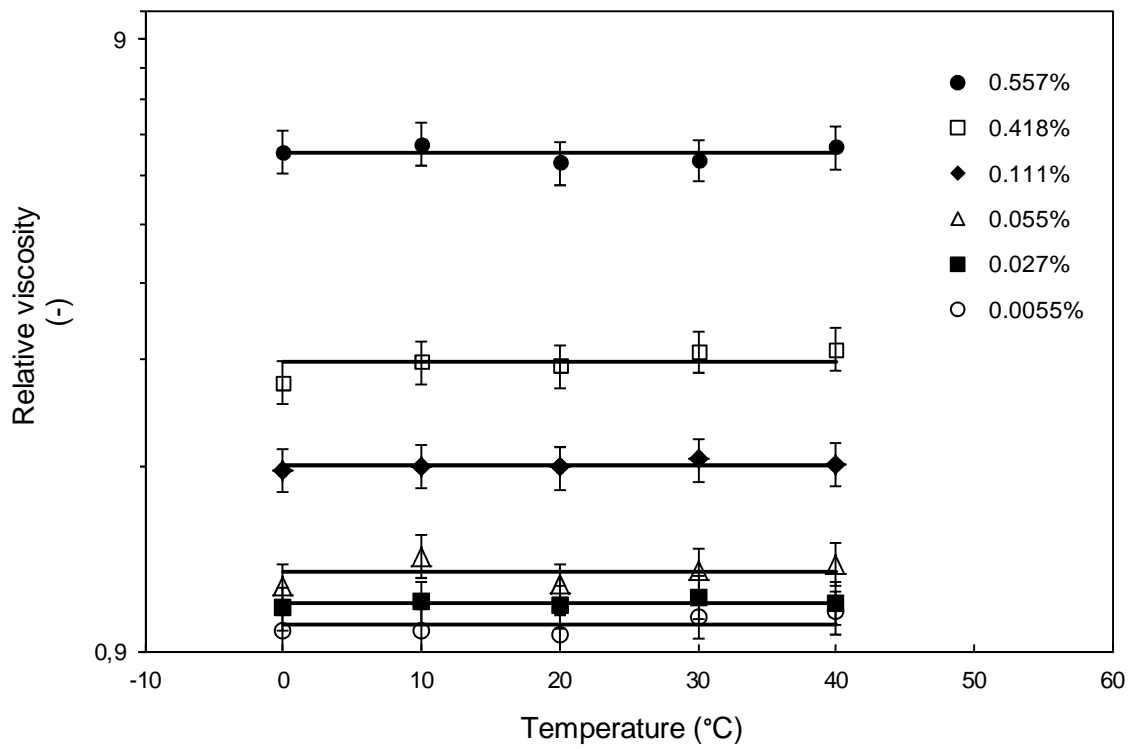


643  
644 Figure 5. Apparent shear viscosity of nanofluid with 0.0055% in CNT volume fraction –  
645 Influence of temperature.  
646



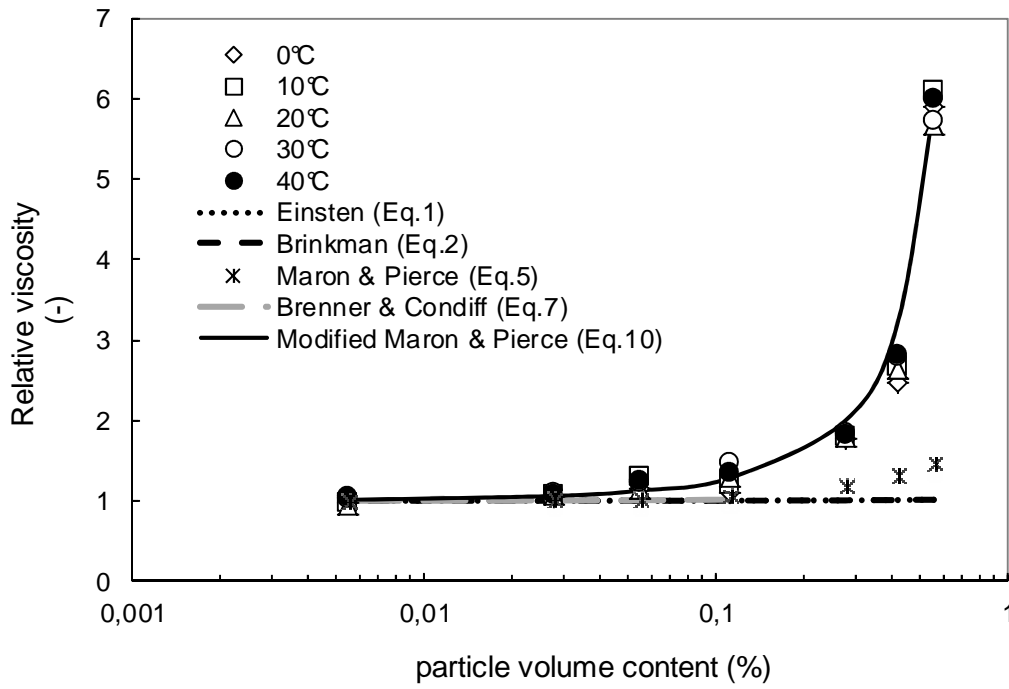
648  
 649 Figure 6. Viscosity of nanofluids at 20°C as a function of shear rate for different volume  
 650 fraction of nanotubes.  
 651





652  
 653  
 654  
 655

Figure 7. Relative viscosity of nanofluids as a function of particle volume content and temperature.



657  
 658  
 659  
 660

Figure 8. Relative viscosity of nanofluids as a function of particle volume content and temperature - Comparison of experimental data and viscosity models.

661 Table 1. Volume fraction of tested nanofluids and corresponding base fluids, and shear  
 662 viscosity of base fluids as a function of SDBS volume fraction and temperatures.  
 663

Volume fraction (%)		Shear viscosity of base fluids (mPa.s)				
CNT	SDBS	0 (°C)	10 (°C)	20 (°C)	30 (°C)	40 (°C)
0.557	1.697	1.98	1.478	1.129	0.877	0.665
0.418	1.272	1.975	1.454	1.102	0.852	0.657
0.278	0.847	1.97	1.401	1.077	0.828	0.648
0.111	0.338	1.964	1.391	1.046	0.799	0.637
0.055	0.169	1.962	1.386	1.036	0.789	0.633
0.0277	0.084	1.961	1.383	1.027	0.784	0.632
0.0055	0.0169	1.96	1.382	1.026	0.780	0.630

664